

# Probing interaction and spatial curvature in the holographic dark energy model

Miao Li,<sup>1,2,\*</sup> Xiao-Dong Li,<sup>3,2,†</sup> Shuang Wang,<sup>4,2,‡</sup> Yi Wang,<sup>5,§</sup> and Xin Zhang<sup>6,1,¶</sup>

<sup>1</sup>Kavli Institute for Theoretical Physics China, Chinese Academy of Sciences, Beijing 100190, China

<sup>2</sup>Key Laboratory of Frontiers in Theoretical Physics, Institute of Theoretical Physics, Chinese Academy of Sciences, Beijing 100190, China

<sup>3</sup>Interdisciplinary Center for Theoretical Study, University of Science and Technology of China, Hefei 230026, China

<sup>4</sup>Department of Modern Physics, University of Science and Technology of China, Hefei 230026, China

<sup>5</sup>Physics Department, McGill University, Montreal, H3A2T8, Canada

<sup>6</sup>Department of Physics, College of Sciences, Northeastern University, Shenyang 110004, China

In this paper we place observational constraints on the interaction and spatial curvature in the holographic dark energy model. We consider three kinds of phenomenological interactions between holographic dark energy and matter, i.e., the interaction term  $Q$  is proportional to the energy densities of dark energy ( $\rho_\Lambda$ ), matter ( $\rho_m$ ), and matter plus dark energy ( $\rho_m + \rho_\Lambda$ ). For probing the interaction and spatial curvature in the holographic dark energy model, we use the latest observational data including the type Ia supernovae (SNIa) Constitution data, the shift parameter of the cosmic microwave background (CMB) given by the five-year Wilkinson Microwave Anisotropy Probe (WMAP5) observations, and the baryon acoustic oscillation (BAO) measurement from the Sloan Digital Sky Survey (SDSS). Our results show that the interaction and spatial curvature in the holographic dark energy model are both rather small. Besides, it is interesting to find that there exists significant degeneracy between the phenomenological interaction and the spatial curvature in the holographic dark energy model.

## I. INTRODUCTION

Observations of type Ia supernovae (SNIa) [1], cosmic microwave background (CMB) [2] and large scale structure (LSS) [3] all indicate the existence of mysterious dark energy driving the current accelerated expansion of universe, and lots of efforts have been made to understand it. The most important theoretical candidate of dark energy is the Einstein's cosmological constant  $\lambda$ , which can fit the observations well so far, but is plagued with the famous fine-tuning and cosmic coincidence problems [4]. Many other dynamical dark energy models have also been proposed in the literature, such as quintessence [5], phantom [6],  $k$ -essence [7], tachyon [8], hessence [9], Chaplygin gas [10], and Yang-Mills condensate [11], etc.

Actually, the dark energy problem may be in essence an issue of quantum gravity [12]. However, by far, we have no a complete theory of quantum gravity, so it seems that we have to consider the effects of gravity in some effective quantum field theory in which some fundamental principles of quantum gravity should be taken into account. It is commonly believed that the holographic principle [13] is just a fundamental principle of quantum gravity. Based on the effective quantum field theory, Cohen et al. [14] pointed out that the quantum zero-point energy of a system with size  $L$  should not exceed the mass of a black hole with the same size, i.e.  $L^3\Lambda^4 \leq LM_{pl}^2$ , where  $\Lambda$  is the ultraviolet (UV) cutoff of the effective quantum field theory, which is closely related to the quantum zero-point energy density, and  $M_{pl} \equiv 1/\sqrt{8\pi G}$  is the reduced Planck mass. This observation relates the UV cutoff of a system to its infrared (IR) cutoff. When we take the whole universe into account, the vacuum energy related to this holographic principle can be viewed as dark energy (its energy density is denoted as  $\rho_\Lambda$  hereafter). The largest IR cutoff  $L$  is chosen by saturating the inequality, so that we get the holographic dark energy density

$$\rho_\Lambda = 3c^2 M_{pl}^2 L^{-2} \quad (1)$$

where  $c$  is a numerical constant characterizing all of the uncertainties of the theory, and its value can only be determined by observations. If we take  $L$  as the size of the current universe, say, the Hubble radius  $H^{-1}$ , then the dark energy density will be close to the observational result. However, Hsu [15] pointed out this yields a wrong equation of state for dark energy. Subsequently, Li [16] suggested to choose the future event horizon of the universe as the IR cutoff of this theory. This choice not only gives a reasonable value for dark energy, but also leads to an accelerated universe. Moreover, the cosmic coincidence problem can also be explained successfully in this model. Most recently, a calculation of the Casimir energy of the photon field in a de Sitter space is performed [17], and it is a surprising result that the Casimir energy is indeed proportional to the size

\*Electronic address: [mli@itp.ac.cn](mailto:mli@itp.ac.cn)

†Electronic address: [renzhe@mail.ustc.edu.cn](mailto:renzhe@mail.ustc.edu.cn)

‡Electronic address: [swang@mail.ustc.edu.cn](mailto:swang@mail.ustc.edu.cn)

§Electronic address: [wangyi@hep.physics.mcgill.ca](mailto:wangyi@hep.physics.mcgill.ca)

¶Electronic address: [zhangxin@mail.neu.edu.cn](mailto:zhangxin@mail.neu.edu.cn)

of the horizon (the usual Casimir energy in a cavity is inversely proportional to the size of the cavity), in agreement with the holographic dark energy model.

The holographic dark energy model has been studied widely [18, 19, 20, 21, 22, 23, 24]. By far, various observational constraints on this model all indicate that the parameter  $c$  is less than 1, implying that the holographic dark energy would lead to a phantom universe with big rip as its ultimate fate [20, 21]. Nevertheless, the appearance of the cosmic doomsday will definitely ruin the theoretical foundation of the holographic dark energy model, namely, the effective quantum field theory; see Ref. [24] for detailed discussions. To evade this difficulty, one may consider the extra dimension effects in this model [24]: The high energy correction from the extra dimensions could erase the big-rip singularity and leads to a de Sitter finale for the holographic cosmos. Another way of avoiding the big rip is to consider some phenomenological interaction between holographic dark energy and matter [22, 23]. With the help of the interaction, the big rip might be avoided due to the occurrence of an attractor solution in which the effective equations of state of dark energy and matter become identical in the far future. However, it should be pointed out that in order to avoid the phantom-like universe the phenomenological interaction term should be tuned to satisfy some specific condition, i.e., the interaction must be strong enough; for detailed discussions see Ref. [23]. The only way of acquiring the knowledge of the interaction strength is from the observational data fitting. In this paper, we will explore the possible phenomenological interactions between holographic dark energy and matter by using the latest observational data.

Another important mission of this paper is to probe the spatial curvature of the universe in the holographic dark energy model. Actually, the current observational data are not accurate enough to distinguish between the dynamical effects of dark energy and spatial curvature of the universe, owing to the degeneracy between them. Indeed, in fitting the equation of state of dark energy,  $w(z)$ , the inclusion of  $\Omega_{k0}$  as an additional parameter would dilute constraints on  $w(z)$ . While most inflation models in which the inflationary periods last for much longer than 60  $e$ -folds predict a spatially flat universe,  $\Omega_{k0} \sim 10^{-5}$ , the current constraint on  $\Omega_{k0}$  is three orders of magnitude larger than this inflation prediction. As argued in Ref. [25], the studies of dark energy, and in particular, of observational data, should include  $\Omega_{k0}$  as a parameter to be fitted alongside the  $w(z)$  parameters. So, in this paper, we will constrain  $\Omega_{k0}$  in the holographic dark energy model in light of the latest observational data. Of course, we will also let the interaction and spatial curvature simultaneously be free parameters, and explore the possible degeneracy between them.

## II. HOLOGRAPHIC DARK ENERGY WITH INTERACTION AND SPATIAL CURVATURE

In this section we shall describe the interacting holographic dark energy in a non-flat universe. In a spatially non-flat Friedmann-Robertson-Walker universe, the Friedmann equation can be written as

$$3M_{pl}^2 \left( H^2 + \frac{k}{a^2} \right) = \rho, \quad (2)$$

where  $\rho = \rho_\Lambda + \rho_m$ . We define

$$\Omega_k = \frac{k}{H^2 a^2} = \Omega_{k0} \left( \frac{H_0}{aH} \right)^2, \quad \Omega_\Lambda = \frac{\rho_\Lambda}{\rho_c}, \quad \Omega_m = \frac{\rho_m}{\rho_c}, \quad (3)$$

where  $\rho_c = 3M_{pl}^2 H^2$  is the critical density of the universe, thus we have

$$1 + \Omega_k = \Omega_m + \Omega_\Lambda. \quad (4)$$

Consider, now, some interaction between holographic dark energy and matter:

$$\dot{\rho}_m + 3H\rho_m = Q, \quad (5)$$

$$\dot{\rho}_\Lambda + 3H(\rho_\Lambda + p_\Lambda) = -Q, \quad (6)$$

where  $Q$  denotes the phenomenological interaction term. Owing to the lack of the knowledge of micro-origin of the interaction, we simply follow other work on the interacting holographic dark energy and parameterize the interaction term generally as  $Q = -3H(b_1\rho_\Lambda + b_2\rho_m)$ , where  $b_1$  and  $b_2$  are the coupling constants. For reducing the complication and the number of parameters, furthermore, we only consider the following three cases: (a)  $b_1 = b$  and  $b_2 = 0$ , (b)  $b_1 = b_2 = b$ , (c)  $b_1 = 0$  and  $b_2 = b$ . We denote the interaction term  $Q$  in these three cases as

$$Q_1 = -3bH\rho_\Lambda, \quad (7)$$

$$Q_2 = -3bH(\rho_\Lambda + \rho_m), \quad (8)$$

$$Q_3 = -3bH\rho_m. \quad (9)$$

For convenience, in the following we uniformly express the interaction term as  $Q_i = -3bH\rho_c\Omega_i$ , where  $\Omega_i = \Omega_\Lambda$ , 1 and  $\Omega_m$ , for  $i = 1, 2$  and 3, respectively. Note that according to our convention  $b < 0$  means that dark energy decays to matter. Moreover, it should be pointed out that  $b > 0$  will lead to unphysical consequences in physics, since  $\rho_m$  will become negative and  $\Omega_\Lambda$  will be greater than 1 in the far future. So, the parameter  $b$  is always assumed to be negative in the literature. However, in the present work, instead of making such an assumption on  $b$ , we let  $b$  be totally free and let the observational data tell us the true story about the holographic dark energy, no matter whether the ultimate fate of the universe is ridiculous or not.

From the definition of holographic dark energy (1), we have

$$\Omega_\Lambda = \frac{c^2}{H^2 L^2}, \quad (10)$$

or equivalently,

$$L = \frac{c}{H\sqrt{\Omega_\Lambda}}. \quad (11)$$

Thus, we easily get

$$\dot{L} = \frac{d}{dt} \left( \frac{c}{H\sqrt{\Omega_\Lambda}} \right) = \left( -\frac{\dot{H}}{H} - \frac{1}{2} \frac{\dot{\Omega}_\Lambda}{\Omega_\Lambda} \right) \frac{c}{H\sqrt{\Omega_\Lambda}}. \quad (12)$$

Following Ref. [18], in a non-flat universe the IR cut-off length scale  $L$  takes the form

$$L = ar(t), \quad (13)$$

and  $r(t)$  satisfies

$$\int_0^{r(t)} \frac{dr}{\sqrt{1-kr^2}} = \int_t^{+\infty} \frac{dt}{a(t)}. \quad (14)$$

Thus, we have

$$r(t) = \frac{1}{\sqrt{k}} \sin \left( \sqrt{k} \int_t^{+\infty} \frac{dt}{a} \right) = \frac{1}{\sqrt{k}} \sin \left( \sqrt{k} \int_{a(t)}^{+\infty} \frac{da}{Ha^2} \right). \quad (15)$$

Equation (13) leads to another equation about  $r(t)$ , namely,

$$r(t) = \frac{L}{a} = \frac{c}{\sqrt{\Omega_\Lambda} Ha}. \quad (16)$$

Combining Eqs. (15) and (16) yields

$$\sqrt{k} \int_t^{+\infty} \frac{dt}{a} = \arcsin \frac{c\sqrt{k}}{\sqrt{\Omega_\Lambda} a H}. \quad (17)$$

Taking derivative of Eq. (17) with respect to  $t$ , one can get

$$\sqrt{\frac{\Omega_\Lambda H^2}{c^2} - \frac{k}{a^2}} = \frac{\dot{\Omega}_\Lambda}{2\Omega_\Lambda} + H + \frac{\dot{H}}{H}. \quad (18)$$

Let us plus Eqs. (5) and (6) together, and then we can obtain the form of  $p_\Lambda$ :

$$\begin{aligned} & (\dot{\rho}_c + \dot{\rho}_k) + 3H(\rho_\Lambda + \rho_m + p_\Lambda) = 0 \\ & \Rightarrow (\dot{\rho}_c + \dot{\rho}_k) + 3H(\rho_c + \rho_k + p_\Lambda) = 0 \\ & \Rightarrow p_\Lambda = -\frac{1}{3H} \left( 2\frac{\dot{H}}{H}\rho_c - 2\frac{\dot{a}}{a}\rho_k \right) - \rho_c - \rho_k. \end{aligned} \quad (19)$$

Substituting  $p_\Lambda$  into Eq. (6), we have

$$\left( 2\frac{\dot{H}}{H} + \frac{\dot{\Omega}_\Lambda}{\Omega_\Lambda} + 3H \right) \rho_\Lambda - H\rho_k - \left( 2\frac{\dot{H}}{H} + 3H \right) \rho_c = 3bH\rho_i, \quad (20)$$

where  $\rho_i$  (with  $i = 1 \sim 3$ ) denotes  $\rho_1 = \rho_\Lambda$ ,  $\rho_2 = \rho_\Lambda + \rho_m = \rho_c + \rho_k$ , and  $\rho_3 = \rho_m = \rho_c + \rho_k - \rho_\Lambda$ , respectively. Divided the above equation by  $\rho_c$ , we get an equation containing  $\dot{H}$  and  $\dot{\Omega}_\Lambda$ ,

$$2(\Omega_\Lambda - 1)\frac{\dot{H}}{H} + \dot{\Omega}_\Lambda + H(3\Omega_\Lambda - 3 - \Omega_k) = 3bH\Omega_i, \quad (21)$$

where  $\Omega_i = \Omega_\Lambda$ ,  $\Omega_\Lambda + \Omega_k$ , and  $1 + \Omega_k - \Omega_\Lambda$ , for  $i = 1, 2$ , and  $3$ , respectively. Combining this equation with Eq. (18), we eventually obtain the following two equations governing the dynamical evolution of the interacting holographic dark energy in a non-flat universe,

$$\frac{1}{H/H_0} \frac{d}{dz} \left( \frac{H}{H_0} \right) = -\frac{\Omega_\Lambda}{1+z} \left( \frac{3\Omega_\Lambda - \Omega_k - 3 - 3b\Omega_i}{2\Omega_\Lambda} - 1 + \sqrt{\frac{\Omega_\Lambda}{c^2} - \frac{\Omega_{k0}(1+z)^2}{(H/H_0)^2}} \right), \quad (22)$$

$$\frac{d\Omega_\Lambda}{dz} = -\frac{2\Omega_\Lambda(1 - \Omega_\Lambda)}{1+z} \left( \sqrt{\frac{\Omega_\Lambda}{c^2} - \frac{\Omega_{k0}(1+z)^2}{(H/H_0)^2}} - 1 - \frac{3\Omega_\Lambda - \frac{(1+z)^2\Omega_{k0}}{(H/H_0)^2} - 3 - 3b\Omega_i}{2(1 - \Omega_\Lambda)} \right). \quad (23)$$

These two equations can be solved numerically and will be used in the data analysis procedure.

### III. OBSERVATIONAL CONSTRAINTS

In the holographic dark energy model with interaction and spatial curvature, there are four free parameters:  $c$ ,  $\Omega_{m0}$ ,  $b$ , and  $\Omega_{k0}$ . In this section, we shall constrain these parameters of the holographic dark energy model by using the latest observational data. For decreasing the complication, let us close some parameters in turn. We shall consider the following four cases: (a) the model of holographic dark energy without interaction and spatial curvature (namely,  $b = 0$  and  $\Omega_{k0} = 0$ ), denoted as HDE; (b) the model of holographic dark energy with spatial curvature but without interaction (namely,  $\Omega_{k0} \neq 0$  but  $b = 0$ ), denoted as KHDE; (c) the model of holographic dark energy with interaction but without spatial curvature (namely,  $b \neq 0$  but  $\Omega_{k0} = 0$ ), denoted as IHDE; (d) the model of holographic dark energy with interaction and spatial curvature (namely,  $b \neq 0$  and  $\Omega_{k0} \neq 0$ ), denoted as KIHDE.

#### A. Observational data used

The observational data we use in this paper include the Constitution SNIa sample, the shift parameter of the CMB given by the five-year Wilkinson Microwave Anisotropy Probe (WMAP5) observations, and the baryon acoustic oscillation (BAO) measurement from the Sloan Digital Sky Survey (SDSS).

##### 1. Type Ia supernovae

For the SNIa data, we use the latest Constitution sample including 397 data that are given in terms of the distance modulus  $\mu_{obs}(z_i)$  compiled in Table 1 of Ref. [26]. The theoretical distance modulus is defined as

$$\mu_{th}(z_i) \equiv 5 \log_{10} D_L(z_i) + \mu_0, \quad (24)$$

where  $\mu_0 \equiv 42.38 - 5 \log_{10} h$  with  $h$  the Hubble constant  $H_0$  in units of 100 km/s/Mpc, and the Hubble-free luminosity distance  $D_L = H_0 d_L$  is

$$D_L(z) = \frac{1+z}{\sqrt{|\Omega_{k0}|}} \text{sinn} \left( \sqrt{|\Omega_{k0}|} \int_0^z \frac{dz'}{E(z')} \right), \quad (25)$$

where  $E(z) \equiv H(z)/H_0$ , and

$$\frac{\text{sinn}(\sqrt{|\Omega_{k0}|}x)}{\sqrt{|\Omega_{k0}|}} = \begin{cases} \sin(\sqrt{|\Omega_{k0}|}x)/\sqrt{|\Omega_{k0}|}, & \text{if } \Omega_{k0} > 0, \\ x, & \text{if } \Omega_{k0} = 0, \\ \sinh(\sqrt{|\Omega_{k0}|}x)/\sqrt{|\Omega_{k0}|}, & \text{if } \Omega_{k0} < 0. \end{cases}$$

TABLE I: Fit results for the holographic dark energy model.

| Model  | $\Omega_{m0}$             | $c$                       | $\Omega_{k0}$                            | $b$                                      | $\chi^2_{min}$ | $\Delta\chi^2_{min}$ |
|--------|---------------------------|---------------------------|--|--|----------------|----------------------|
| HDE    | $0.277^{+0.022}_{-0.021}$ | $0.818^{+0.113}_{-0.097}$ |  |  | 465.912        | 0                    |
| KHDE   | $0.278^{+0.037}_{-0.035}$ | $0.815^{+0.179}_{-0.139}$ | $(7.7 \times 10^{-4})^{+0.018}_{-0.019}$ |  | 465.906        | 0.006                |
| IHDE1  | $0.277^{+0.035}_{-0.034}$ | $0.818^{+0.197}_{-0.257}$ |  | $(6.1 \times 10^{-5})^{+0.036}_{-0.025}$ | 465.911        | 0.001                |
| IHDE2  | $0.277^{+0.034}_{-0.036}$ | $0.816^{+0.170}_{-0.223}$ |  | $(1.6 \times 10^{-4})^{+0.009}_{-0.008}$ | 465.910        | 0.002                |
| IHDE3  | $0.277^{+0.034}_{-0.036}$ | $0.815^{+0.164}_{-0.209}$ |  | $(3.0 \times 10^{-4})^{+0.011}_{-0.011}$ | 465.909        | 0.003                |
| KIHDE1 | $0.281^{+0.047}_{-0.043}$ | $0.977^{+0.563}_{-0.551}$ | $0.030^{+0.066}_{-0.127}$                | $-0.046^{+0.243}_{-0.107}$               | 465.697        | 0.315                |
| KIHDE2 | $0.281^{+0.047}_{-0.044}$ | $0.974^{+0.559}_{-0.475}$ | $0.030^{+0.070}_{-0.100}$                | $-0.042^{+0.191}_{-0.073}$               | 465.700        | 0.312                |
| KIHDE3 | $0.280^{+0.045}_{-0.042}$ | $0.961^{+0.231}_{-0.499}$ | $0.061^{+0.038}_{-0.210}$                | $-0.048^{+0.113}_{-0.042}$               | 465.719        | 0.293                |

The  $\chi^2$  for the SNIa data is

$$\chi^2_{SN} = \sum_{i=1}^{397} \frac{[\mu_{obs}(z_i) - \mu_{th}(z_i)]^2}{\sigma_i^2}, \quad (26)$$

where  $\mu_{obs}(z_i)$  and  $\sigma_i$  are the observed value and the corresponding  $1\sigma$  error of distance modulus for each supernova, respectively.

## 2. Baryon acoustic oscillation

For the BAO data, we consider the parameter  $A$  from the measurement of the BAO peak in the distribution of SDSS luminous red galaxies, which is defined as [27]

$$A \equiv \frac{\sqrt{\Omega_{m0}}}{E(z_b)^{\frac{1}{3}}} \left[ \frac{1}{z_b \sqrt{|\Omega_{k0}|}} \text{sinn} \left( \sqrt{|\Omega_{k0}|} \int_0^{z_b} \frac{dz'}{E(z')} \right) \right]^{\frac{2}{3}}, \quad (27)$$

where  $z_b = 0.35$ . The SDSS BAO measurement [27] gives  $A_{obs} = 0.469 (n_s/0.98)^{-0.35} \pm 0.017$ , where the scalar spectral index is taken to be  $n_s = 0.960$  as measured by WMAP5 [28]. It is widely believed that  $A$  is nearly model independent and can provide robust constraint as complement to SNIa data. The  $\chi^2$  for the BAO data is

$$\chi^2_{BAO} = \frac{(A - A_{obs})^2}{\sigma_A^2}, \quad (28)$$

where the corresponding  $1\sigma$  error is  $\sigma_A = 0.017$ .

## 3. Cosmic microwave background

For the CMB data, we use the CMB shift parameter  $R$  given by [29, 30]

$$R \equiv \frac{\sqrt{\Omega_{m0}}}{\sqrt{|\Omega_{k0}|}} \text{sinn} \left( \sqrt{|\Omega_{k0}|} \int_0^{z_{rec}} \frac{dz'}{E(z')} \right), \quad (29)$$

where the redshift of recombination  $z_{rec} = 1090$  [28]. The shift parameter  $R$  relates the angular diameter distance to the last scattering surface, the comoving size of the sound horizon at  $z_{rec}$  and the angular scale of the first acoustic peak in CMB power spectrum of temperature fluctuations [29, 30]. The current measured value of  $R$  is  $R_{obs} = 1.710 \pm 0.019$  from WMAP5 [28]. It should be noted that, different from the SNIa and BAO data, the  $R$  parameter can provide the information about the universe at very high redshift. The  $\chi^2$  for the CMB data is

$$\chi^2_{CMB} = \frac{(R - R_{obs})^2}{\sigma_R^2}, \quad (30)$$

where the corresponding  $1\sigma$  error is  $\sigma_R = 0.019$ .

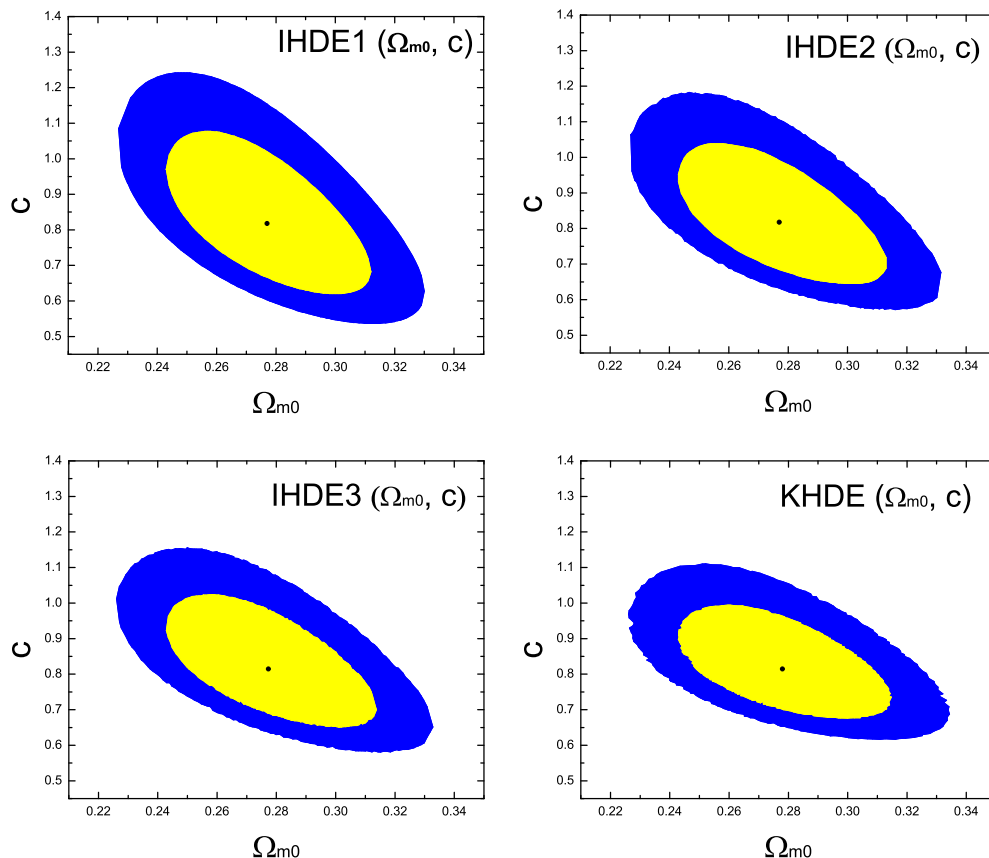


FIG. 1: Probability contours at 68.3% and 95.4% confidence levels in the  $\Omega_{m0} - c$  plane, for the three IHDE models and the KHDE model.

## B. Results and discussions

Table I summarizes the fit results for the considered models. In this table we show the best-fit and  $1\sigma$  values of the parameters and the  $\chi^2_{min}$  of the models. Here,  $\Delta\chi^2_{min} = \chi^2_{min}(\text{HDE}) - \chi^2_{min}$  stands for the improvement of the model in  $\chi^2_{min}$  comparing to the HDE model. From this table, one can find two significant features. One feature is that for the KHDE and IHDE models the values of  $\Delta\chi^2_{min}$  are rather small, and their best-fit parameters (namely,  $\Omega_{m0}$  and  $c$ ) are very close to the corresponding ones in the HDE model. The best-fit values and  $1\sigma$  regions of  $\Omega_{k0}$  and  $b$  are fairly small, implying that the holographic dark energy model prefers zero curvature and zero interaction. The other feature is that for the KIHDE models  $\Delta\chi^2_{min}$  as well as the best-fit and  $1\sigma$  values of  $\Omega_{k0}$  and  $b$  are much larger than those in the KHDE and IHDE models. This indicates that there possibly exists some strong degeneracy between the spatial curvature and the interaction in the holographic dark energy model. Also, the best-fit values and  $1\sigma$  ranges of  $c$  in the KIHDE models become remarkably larger than those in other cases.

Figures 1–5 show the probability contours at 68.3% and 95.4% confidence levels (CL) in various parameter planes for these models. Let us discuss the various cases in detail in what follows.

In Fig. 1, we plot the  $1\sigma$  and  $2\sigma$  contours in the  $\Omega_{m0} - c$  plane for the KHDE and IHDE models. We see from this figure that the inclusion of spatial curvature or interaction in the holographic dark energy makes the parameter space of  $(\Omega_{m0}, c)$  become larger. For the HDE model, we have  $c < 1$  in about  $2\sigma$  range, for details see Fig. 1 of Ref. [21]. However, when considering the spatial curvature or the interaction, we can only obtain  $c < 1$  in about  $1\sigma$  range. In fact, in the IHDE models  $c$  could be evidently greater than one even in the  $1\sigma$  range. This, in some sense, is good news for the fate of the universe because the likelihood of holographic dark energy becoming a phantom decreases. The negative aspect lies in that the uncertainty is enlarged owing to the amplification of the parameter space.

Figures 2 and 3 show the degeneracy situations of  $b$  and  $\Omega_{m0}$ , as well as  $b$  and  $c$ , in the IHDE models. It is clear that  $b$  and  $\Omega_{m0}$  are in positive correlation, and  $b$  and  $c$  are anti-correlated. From these two figures one can see that the observational data tell us that  $b$  can be both positive and negative. In our convention, a positive  $b$  will lead to an unphysical future for the universe since  $\rho_m$  will become negative and  $\Omega_\Lambda$  will be greater than one in the far future. So, one should only consider the regions of  $b \leq 0$  in the figures as realistic physical situations. The best-fit values for  $b$  are all close to zero, although slightly larger than zero. Concretely,  $b = 6.1 \times 10^{-5}$ ,  $1.6 \times 10^{-4}$  and  $3.0 \times 10^{-4}$ , for the three IHDE models, respectively. The 95% CL limits on  $b$

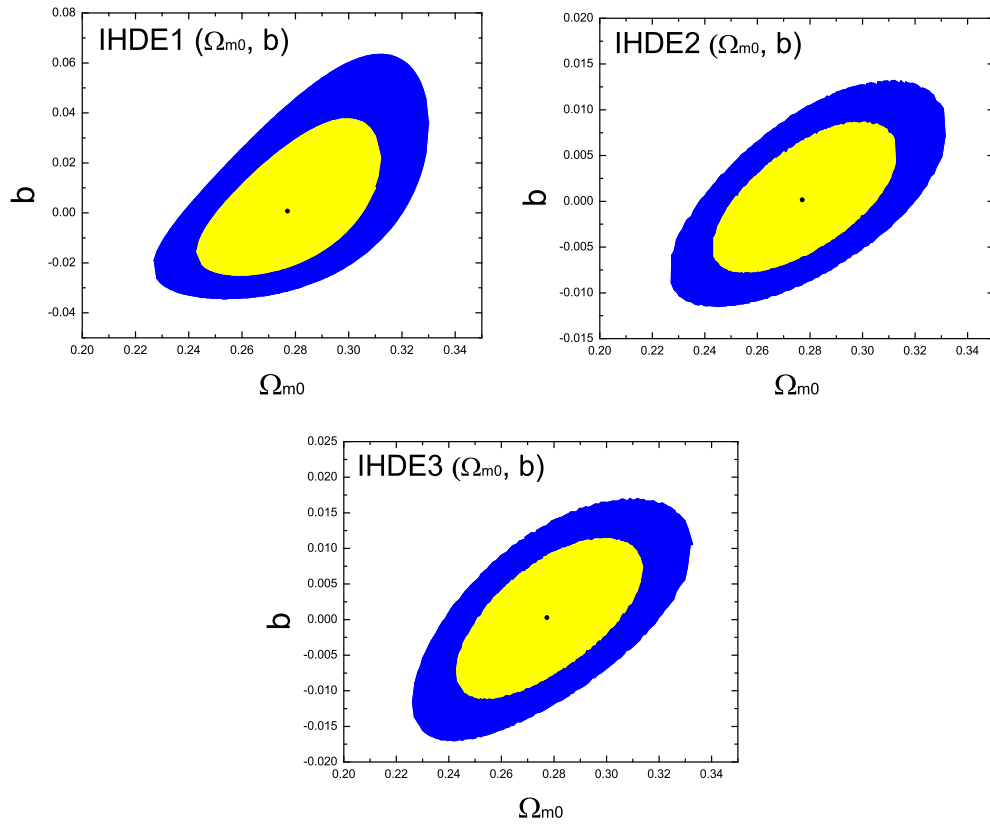


FIG. 2: Probability contours at 68.3% and 95.4% confidence levels in the  $\Omega_{m0} - b$  plane, for the three IHDE models.

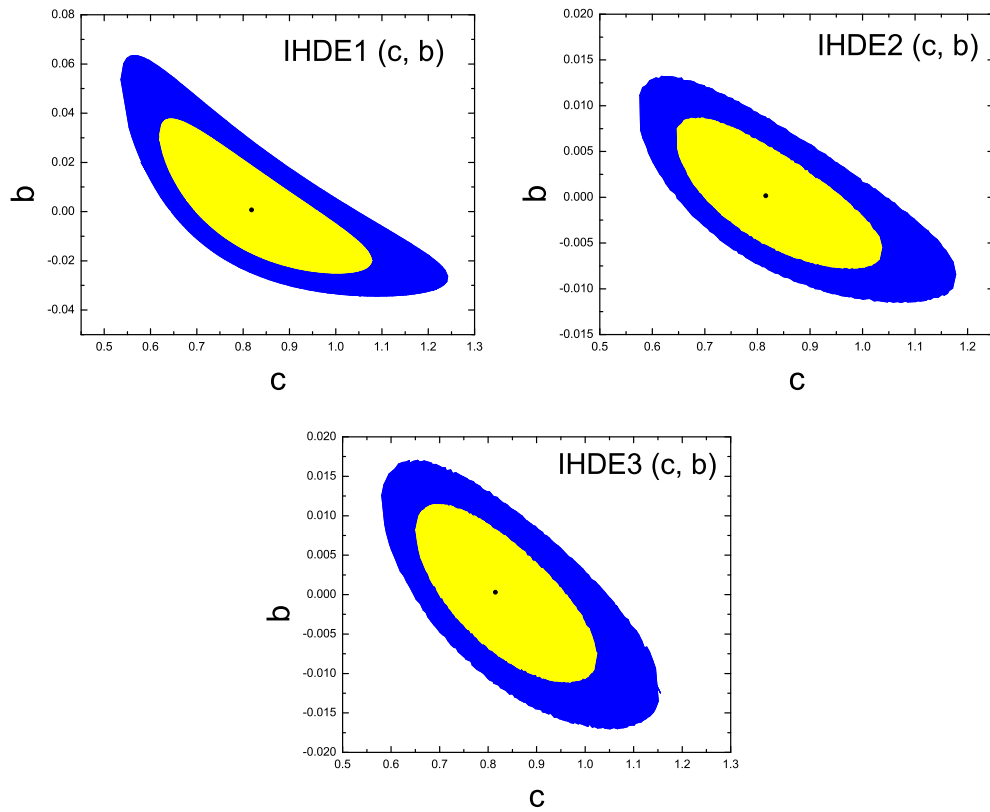


FIG. 3: Probability contours at 68.3% and 95.4% confidence levels in the  $c - b$  plane, for the three IHDE models.

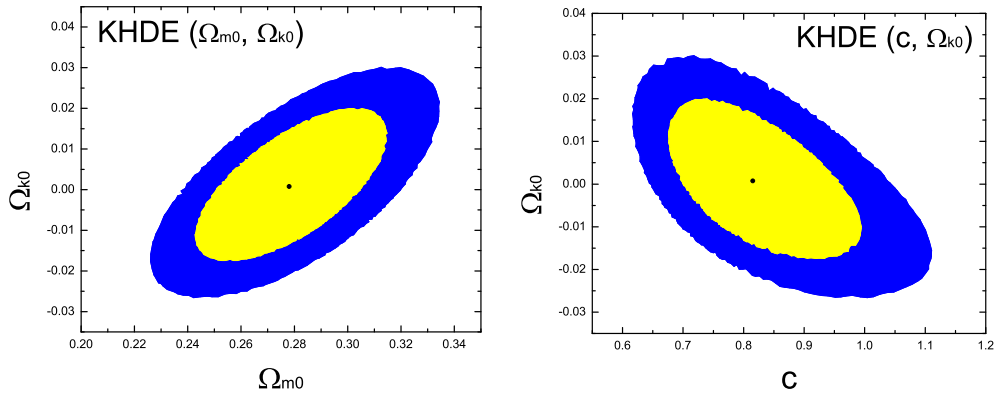


FIG. 4: Probability contours at 68.3% and 95.4% confidence levels in the  $\Omega_{m0} - \Omega_{k0}$  and  $c - \Omega_{k0}$  planes, for the KHDE model.

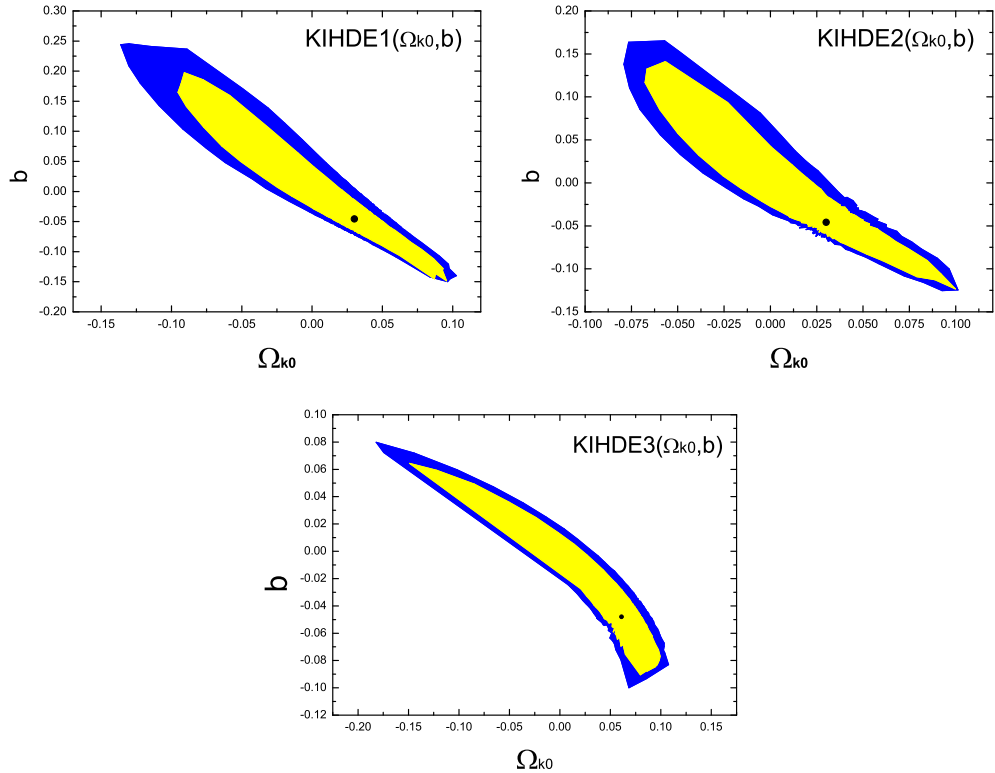


FIG. 5: Probability contours at 68.3% and 95.4% confidence levels in the  $\Omega_{k0} - b$  planes, for the three KIHDE models.

are fairly small, in order of  $10^{-2}$ . This indicates that the observations do not favor an interacting holographic dark energy model. However, it should be pointed out that even a small  $b$  could possibly be used to avoid the future big rip caused by  $c < 1$ . The sufficient and necessary condition of avoiding the big rip in the interacting holographic dark energy model with  $c < 1$  has been studied in detail in Ref. [23]. According to this work, we know that: for IHDE1, the condition is  $b \leq 1 - c^{-2}$ ; for IHDE2, the condition is  $b \leq c^2 - 1$ ; for IHDE3, there is no late-time attractor solution, so the big rip will be inevitable. From Fig. 3, we find that for IHDE1 and IHDE2 the points satisfying such sufficient and necessary conditions of avoiding the big rip actually could be found in the 95% CL region with  $b < 0$  and  $c < 1$ .

The constraints on KHDE from the latest SNIa, CMB and BAO data are shown in Fig. 4. The left panel shows that  $\Omega_{k0}$  and  $\Omega_{m0}$  are in positive correlation, and the right panel indicates that  $\Omega_{k0}$  and  $c$  are anti-correlated. The best-fit value for  $\Omega_{k0}$  is  $7.7 \times 10^{-4}$ , quite close to zero. The values of  $\Omega_{k0}$  in  $2\sigma$  region can be both positive and negative. The 95% CL limit on  $\Omega_{k0}$  is in order of  $10^{-2}$ , nearly as good as that for a vacuum energy model. These results indicate that the observations actually favor a spatially flat holographic dark energy model.

Furthermore, we consider the most sophisticated case for the holographic dark energy model, i.e., the interacting holographic

dark energy in a non-flat universe. Figure 5 shows the constraints on  $b$  and  $\Omega_{k0}$  of the KIHDE models from the latest SN, CMB and BAO data. We find that  $b$  and  $\Omega_{k0}$  are strongly anti-correlated. It is remarkable that there exists significant degeneracy between the phenomenological interaction and spatial curvature in the holographic dark energy model. When simultaneously considering the interaction and spatial curvature in the holographic dark energy model, the parameter space is amplified, especially, the ranges of  $b$  and  $\Omega_{k0}$  are enlarged by 10 times comparing to the IHDE and KHDE models. From Fig. 5, we find that the holographic dark energy model with zero interaction and flat geometry is still favored. Of course, the best-fit points all indicate an interacting holographic dark energy (with  $b$  about  $-0.05$ ) in a closed universe. When imposing the physical condition  $b < 0$ , one can find from Fig. 5 that a closed geometry is more favored.

Finally, we feel that it would be better to make some additional comments on the other related work of interacting holographic dark energy models. In an early work [31], the interacting holographic dark energy model (namely, the case of IHDE2) was first proposed; subsequently, this model was constrained by using the observational data of that time [32]. Comparing with these earlier studies, our results show a significant reduction of the errors of parameters, owing to the more accurate data used. It should also be mentioned that in Ref. [33] the interaction between holographic dark energy and matter was reconstructed by employing two commonly used parametrization form for the equation of state of dark energy. In addition, the interacting holographic dark energy models with the Hubble scale as IR cutoff were also discussed in, e.g., Refs. [34, 35]. The interacting holographic dark energy model in a spatially closed universe was investigated in Ref. [36] where an additional requirement that the entropy attributed to the IR cutoff  $L$  should be increasing was imposed. However, in the present paper, such a condition is not imposed since an appropriate definition of entropy for a holographic universe is still obscure for us (some studies show that the Friedmann equation is consistent with the first law of thermodynamics of the apparent horizon, see, e.g., Refs. [37, 38]). It should also be noted that there are some other versions of holographic dark energy model, for example, the agegraphic dark energy model [39, 40, 41] and the Ricci dark energy model [42, 43]. The interacting agegraphic dark energy model has been discussed [44], but the interacting version of Ricci dark energy model has not been investigated.

#### IV. CONCLUSION

In this paper we consider a sophisticated holographic dark energy model where the interaction and spatial curvature are both involved. The consideration of interaction between dark energy and matter in the holographic dark energy is rather popular, since the interaction not only can help to alleviate the cosmic coincidence problem but also can be used to avoid the future big-rip singularity caused by  $c < 1$ . In addition, the consideration of spatial geometry in the holographic dark energy is also necessary, because usually there exists some degeneracy between the spatial curvature and the dynamics of dark energy. The aim of this paper is to probe the possible interaction and spatial curvature in the holographic dark energy model in light of the latest observational data.

We considered three kinds of phenomenological interactions between holographic dark energy and matter, i.e., the interaction term  $Q$  is proportional to the energy densities of dark energy ( $\rho_\Lambda$ ), matter ( $\rho_m$ ) and dark energy plus matter ( $\rho_\Lambda + \rho_m$ ). For the observational data, we used the SNIa Constitution data, the shift parameter  $R$  of the CMB from the WMAP5, and the BAO parameter  $A$  from the SDSS. We separately considered the following cases: opening interaction but closing spatial curvature; opening spatial curvature but closing interaction; simultaneously opening interaction and spatial curvature. Our results show that when separately considering the interaction and spatial curvature, the interaction and spatial curvature in the holographic dark energy model are both rather small. In other words, the observations favor a non-interacting holographic dark energy with flat geometry. When considering both the interaction and the spatial curvature in the holographic dark energy model, it is interesting to find that there exists remarkable degeneracy between them. On the whole, according to the current observational data, the holographic dark energy model without interaction and spatial curvature is still more favored.

#### Acknowledgments

This work was supported by the Natural Science Foundation of China under Grants Nos. 10705041, 10821504, 10975032 and 10975172, and Ministry of Science and Technology 973 program under Grant No. 2007CB815401. SW also thanks the support from a graduate fund of the University of Science and Technology of China.

- 
- [1] A.G. Riess *et al.*, *Astron.J.* **116**, 1009 (1998); S. Perlmutter *et al.*, *ApJ* **517**, 565 (1999); J. L. Tonry *et al.*, *ApJ* **594**, 1 (2003); R.A. Knop *et al.*, *ApJ* **598**, 102 (2003); A.G. Riess *et al.*, *ApJ* **607**, 665 (2004).  
[2] D.N. Spergel *et al.*, *ApJS* **148**, 175 (2003); C.L. Bennet *et al.*, *ApJS*. **148**, 1 (2003); D.N. Spergel *et al.*, *ApJS* **170**, 377 (2007); L. Page *et al.*, *ApJS* **170**, 335 (2007); G. Hinshaw *et al.*, *ApJS* **170**, 263 (2007).

- [3] M. Tegmark *et al.*, Phys. Rev. **D69**, 103501 (2004); ApJ **606**, 702 (2004); Phys. Rev. **D74**, 123507 (2006).
- [4] S. Weinberg, Rev. Mod. Phys. **61**, 1 (1989); arXiv:astro-ph/0005265; V. Sahni and A.A. Starobinsky, Int. J. Mod. Phys. **D 9**, 373 (2000); S.M. Carroll, Living Rev. Rel. **4**, 1 (2001); P.J.E. Peebles and B. Ratra, Rev. Mod. Phys. **75**, 559 (2003); T. Padmanabhan, Phys. Rept. **380**, 235 (2003); V. Sahni, Lect. Notes Phys. **653**, 141 (2004); E. J. Copeland, M. Sami and S. Tsujikawa, Int. J. Mod. Phys. **D 15**, 1753 (2006); J. Frieman, M. Turner and D. Huterer, Ann. Rev. Astron. Astrophys. **46**, 385 (2008).
- [5] B. Ratra and P.J.E. Peebles, Phys. Rev. **D37**, 3406 (1988); P.J.E. Peebles and B. Ratra, ApJ **325**, L17 (1988); C. Wetterich, Nucl. Phys. **B302**, 668 (1988); A&A **301**, 321 (1995); R.R. Caldwell, R. Dave and P.J. Steinhardt, Phys. Rev. Lett. **80**, 1582 (1998); I. Zlatev, L. Wang and P.J. Steinhardt Phys. Rev. Lett. **82**, 896 (1999).
- [6] R.R. Caldwell, Phys. Lett. B **545**, 23 (2002); S.M. Carroll, M. Hoffman and M. Trodden, Phys. Rev. **D68**, 023509 (2003); R.R. Caldwell, M. Kamionkowski and N.N. Weinberg, Phys. Rev. Lett. **91**, 071301 (2003).
- [7] C. Armendariz-Picon, T. Damour and V. Mukhanov, Phys. Lett. B **458**, 209 (1999); C. Armendariz-Picon, V. Mukhanov and P.J. Steinhardt, Phys. Rev. **D63**, 103510 (2001); T. Chiba, T. Okabe and M. Yamaguchi, Phys. Rev. **D62**, 023511 (2000).
- [8] T. Padmanabhan, Phys. Rev. **D66**, 021301 (2002); J.S. Bagla, H.K. Jassal, and T. Padmanabhan, Phys. Rev. **D67**, 063504 (2003).
- [9] H. Wei, R.G. Cai, and D.F. Zeng, Class. Quant. Grav. **22**, 3189 (2005); H. Wei, and R.G. Cai, Phys. Rev. **D72**, 123507 (2005); H. Wei, N.N. Tang, and R.G. Cai, Phys. Rev. **D75**, 043009 (2007).
- [10] A.Y. Kamenshchik, U. Moschella and V. Pasquier, Phys. Lett. B **511**, 265 (2001); M.C. Bento, O. Bertolami and A.A. Sen, Phys. Rev. D **66**, 043507 (2002); X. Zhang, F.Q. Wu and J. Zhang, JCAP **0601**, 003 (2006).
- [11] W. Zhao and Y. Zhang, Class. Quant. Grav. **23**, 3405 (2006); T.Y. Xia and Y. Zhang, Phys. Lett. B **656**, 19 (2007); S. Wang, Y. Zhang and T.Y. Xia, JCAP **10** 037 (2008); S. Wang and Y. Zhang, Phys. Lett. B **669** 201(2008).
- [12] E. Witten, arXiv:hep-ph/0002297.
- [13] G. 't Hooft, gr-qc/9310026; L. Susskind, J. Math. Phys. **36**, 6377 (1995); J. D. Bekenstein, Phys. Rev. D **7**, 2333 (1973); J. D. Bekenstein, Phys. Rev. D **9**, 3292 (1974); J. D. Bekenstein, Phys. Rev. D **23**, 287 (1981); J. D. Bekenstein, Phys. Rev. D **49**, 1912(1994); S. W. Hawking, Commun. Math. Phys. **43**, 199 (1975); S. W. Hawking, Phys. Rev. D **13**, 191 (1976).
- [14] A. G. Cohen, D. B. Kaplan and A. E. Nelson, Phys. Rev. Lett. **82**, 4971 (1999).
- [15] S. D. H. Hsu, Phys. Lett. B **594**, 13 (2004).
- [16] M. Li, Phys. Lett. B **603**, 1 (2004).
- [17] M. Li, M. X. Miao and Y. Pang, arXiv:0910.3375.
- [18] Q. G. Huang and M. Li, JCAP **0408**, 013 (2004).
- [19] Q. G. Huang and M. Li, JCAP **0503**, 001 (2005); X. Zhang, Int. J. Mod. Phys. D **14**, 1597 (2005); Phys. Lett. B **648**, 1 (2007); Phys. Rev. D **74**, 103505 (2006); B. Chen, M. Li and Y. Wang, Nucl. Phys. B **774**, 256 (2007); J.F. Zhang, X. Zhang and H.Y. Liu, Eur. Phys. J. C **52**, 693 (2007); Phys. Lett. B **651**, 84 (2007); H. Wei and S.N. Zhang, Phys. Rev. D **76**, 063003 (2007); C.J. Feng, Phys. Lett. B **633**, 367 (2008); Y. Z. Ma and X. Zhang, Phys. Lett. B **661**, 239 (2008); M. Li, X.D. Li, C. Lin and Y. Wang, Commun. Theor. Phys. **51**, 181 (2009); Y.G. Gong and T.J. Li, arXiv:0907.0860; S. Nojiri and S. D. Odintsov, Gen. Rel. Grav. **38**, 1285 (2006).
- [20] Q. G. Huang and Y. G. Gong, JCAP **0408**, 006 (2004); X. Zhang and F. Q. Wu, Phys. Rev. D **72**, 043524 (2005); Phys. Rev. D **76**, 023502 (2007); Z. Chang, F. Q. Wu and X. Zhang, Phys. Lett. B **633**, 14 (2006); J. Y. Shen, B. Wang, E. Abdalla and R. K. Su, Phys. Lett. B **609**, 200 (2005); Z. L. Yi and T. J. Zhang, Mod. Phys. Lett. A **22**, 41 (2007); Y. Z. Ma, Y. Gong and X. Chen, Eur. Phys. J. C **60**, 303 (2009).
- [21] M. Li, X. D. Li, S. Wang and X. Zhang, JCAP **0906**, 036 (2009).
- [22] B. Wang, C. Y. Lin and E. Abdalla, Phys. Lett. B **637**, 357 (2006); B. Wang, C. Y. Lin, D. Pavon and E. Abdalla, Phys. Lett. B **662**, 1 (2008); J. Zhang, X. Zhang and H. Liu, Phys. Lett. B **659**, 26 (2008); H. M. Sadjadi and M. Honardoost, Phys. Lett. B **647**, 231 (2007).
- [23] M. Li, C. Lin and Y. Wang, JCAP **0805**, 023 (2008).
- [24] X. Zhang, arXiv:0909.4940.
- [25] C. Clarkson, M. Cortes and B. A. Bassett, JCAP **0708**, 011 (2007).
- [26] M. Hicken *et al.*, Astrophys. J. **700**, 1097 (2009).
- [27] D.J. Eisenstein *et al.*, ApJ. **633**, 560 (2005).
- [28] E. Komatsu *et al.*, ApJS. **180**, 3301 (2009).
- [29] J.R. Bond, G. Efstathiou and M. Tegmark, MNRAS. **291**, L33 (1997).
- [30] Y. Wang and P. Mukherjee, ApJ. **650**, 1 (2006).
- [31] B. Wang, Y. Gong and E. Abdalla, Phys. Lett. B **624**, 141 (2005).
- [32] C. Feng, B. Wang, Y. Gong and R. K. Su, JCAP **0709**, 005 (2007); Q. Wu, Y. Gong, A. Wang and J. S. Alcaniz, Phys. Lett. B **659**, 34 (2008); K. Karwan, JCAP **0805**, 011 (2008).
- [33] S. F. Wu, P. M. Zhang and G. H. Yang, Class. Quant. Grav. **26**, 055020 (2009).
- [34] N. Cruz, S. Lepe, F. Pena and J. Saavedra, Phys. Lett. B **669**, 271 (2008).
- [35] L. Xu, JCAP **0909**, 016 (2009).
- [36] H. Mohseni Sadjadi and N. Vadood, JCAP **0808**, 036 (2008).
- [37] R. G. Cai and S. P. Kim, JHEP **0502**, 050 (2005).
- [38] R. G. Cai and L. M. Cao, Phys. Rev. D **75**, 064008 (2007); R. G. Cai and L. M. Cao, Nucl. Phys. B **785**, 135 (2007); Y. Gong and A. Wang, Phys. Rev. Lett. **99**, 211301 (2007); Y. Gong, B. Wang and A. Wang, JCAP **0701**, 024 (2007); R. G. Cai, L. M. Cao and Y. P. Hu, Class. Quant. Grav. **26**, 155018 (2009).
- [39] R. G. Cai, Phys. Lett. B **657**, 228 (2007).
- [40] H. Wei and R. G. Cai, Phys. Lett. B **660**, 113 (2008).
- [41] X. Wu, Y. Zhang, H. Li, R. G. Cai and Z. H. Zhu, arXiv:0708.0349; H. Wei and R. G. Cai, Phys. Lett. B **663**, 1 (2008); I. P. Neupane, Phys. Rev. D **76**, 123006 (2007); J. Zhang, X. Zhang and H. Liu, Eur. Phys. J. C **54**, 303 (2008); Y. W. Kim, H. W. Lee, Y. S. Myung and M. I. Park, Mod. Phys. Lett. A **23**, 3049 (2008). J. P. Wu, D. Z. Ma and Y. Ling, Phys. Lett. B **663**, 152 (2008); J. Cui, L. Zhang, J. Zhang and X. Zhang, arXiv:0902.0716; X. L. Liu and X. Zhang, Commun. Theor. Phys. **52**, 761 (2009).

- [42] C. Gao, F. Q. Wu, X. Chen and Y. G. Shen, Phys. Rev. D **79**, 043511 (2009).
- [43] C. J. Feng, arXiv:0806.0673; C. J. Feng, Phys. Lett. B **670**, 231 (2008); C. J. Feng, Phys. Lett. B **672**, 94 (2009); X. Zhang, Phys. Rev. D **79**, 103509 (2009); L. Xu, W. Li and J. Lu, arXiv:0810.4730; C. J. Feng, arXiv:0812.2067; K. Y. Kim, H. W. Lee and Y. S. Myung, arXiv:0812.4098. R. G. Cai, B. Hu and Y. Zhang, Commun. Theor. Phys. **51**, 954 (2009). C. J. Feng and X. Zhang, Phys. Lett. B **680**, 399 (2009); L. N. Granda, W. Cardona and A. Oliveros, arXiv:0910.0778.
- [44] L. Zhang, J. Cui, J. Zhang and X. Zhang, arXiv:0911.2838; A. Sheykhi, Phys. Lett. B **680**, 113 (2009).